Detection of the degraded interface in dissymmetrical glued structures using Lamb waves

Latifa Attar, Damien Leduc, Mounsif Ech Cherif El Kettani, Mihai Valentin Predoi, Jocelyne Galy, Pascal Pareige

Detection of the degraded interface in dissymmetrical glued structures using Lamb waves

Latifa Attar[a], Damien Leduc[a,*], Mounsif Ech Cherif El Kettani[a], Mihai Valentin Predoi[b], Jocelyne Galy[c], Pascal Pareige[a]

[a] *Laboratoire Ondes et Milieux Complexes (LOMC), UMR CNRS 6294, University of Normandy, 75 rue Bellot, 76600 Le Havre, France*

[b] *Department of Mechanics, University Politehnica of Bucharest, Splaiul Independentei, 313, sect. 6, Bucarest, 060042 Bucarest, Romania*

[c] *Laboratoire Ingénierie des Matériaux Polymères (IMP), UMR CNRS 5223, INSA Lyon, Bâtiment Jules Verne 17, avenue Jean Capelle, 69621 Villeurbanne, France*

* Corresponding author.
E-mail address: damien.leduc@univ-lehavre.fr (D. Leduc).

Abstract

Structural bonds, particularly the ones made of composite materials, have many advantages over other assembly methods. The progress in mastering these two complementary technologies (i.e. structural bonding and composite materials), has made it possible to consider their use in many industrial fields including aeronautics and automobile. Many references exist on bonding quality assessment, but none was addressing the identification of degraded adhesive interface. This work presents numerical and experimental results on the evaluation of the quality of bonding in a metal/adhesive/carbon-epoxy composite structure using Lamb guided waves. For two studied samples, only one of the two interfaces has its bonding quality degraded by inserting a release agent while keeping a good adhesion for the other interface (adhesive degradation). For one other sample, the cross-linking of the epoxy adhesive is partial (cohesive degradation). A numerical study, based on the semi-analytical finite element method (SAFE), is performed. The SAFE model uses extremely thin elastic layers, called interphases, between the adhesive and the plates, which enable an investigation of the bonding quality. Various samples with very different adhesion levels, indicated by a parameter related to the interphase, are investigated and a data base of dispersion curves is thus obtained. An experimental study, based on generation of waves by a piezocomposite transducer and reception by a laser vibrometer, is then performed to plot the experimental dispersion curves. On each experimental result, numerically computed Lamb dispersion curves are superimposed, and the most adequate value of the adhesion quality parameter for each interphase is determined. The different samples quality can be thus identified. Moreover, it is possible to identify on which interface (metal/adhesive or composite/adhesive interface) the quality of the adhesion is degraded.

1.   Introduction

Composite materials have been extensively used over the past decades in primary structural applications as well as in aeronautics and automobile industries in which a gradual replacement process of some metal/metal structures by metal/composite structures is in progress. There are indeed several reasons that encourage manufacturers to turn to bonded assemblies [1-3] rather than traditional ones (riveting, bolting). Bonding makes it possible to assemble different, soft, flexible or fragile materials. It enables a weight reduction and a better distribution of the mechanical strain on the whole structure. However, this technology is still relatively recent and systematic evaluation of the mechanical strength of bonded assemblies is necessary. For example, current aviation regulations still require the use of traditional fasteners in the absence of reliable control of the glued assembly.

Ultrasonic nondestructive evaluation techniques were used by many researchers to characterize the adhesion quality between two substrates. Ultrasonic guided waves are a recent promising alternative, as a particular case of ultrasonic waves which are widely used in non-destructive testing and evaluation (NDT/NDE) [4-6]. Bulk longitudinal [7] and shear waves, as well as Lamb [8-10] and shear horizontal (SH) guided waves [11,12] have been used to investigate the bonding quality. Adams and Drinkwater classified the main bonding defects and their detectability [13]. Many authors [14-18] used Lamb-type waves due to their relatively long propagation distance. Detectability of kissing bonds [19], overlapping plates [20] or defects in bonded mechanical parts [21] were also addressed.

Different research projects are devoted to the subject of quality bond assurance. For example, there were the European project ENCOMB (Extended Non-Destructive Testing of Composite Bonds) and the French project ANR ISABEAU (Innovating for Structural Adhesive Bonding Evaluation and Analysis with Ultrasounds, ANR-12-BS09-0022). The

objective of the ENCOMB project (2010-2014) was the development and adaptation of extended non-destructive testing (ENDT) methods for pre- and post-bond inspection of CFRP aircraft structural components. Different techniques were used: nonlinear ultrasound, laser ultrasound, laser-induced shock experiments and active thermography. However Lamb-wave based approaches were not exploited extensively so far: these approaches have shown good sensitivity to water contamination [22]. The goal of the ANR ISABEAU project (2013-2017) was to study the verification of the integrity of adhesively bonded joints using ultrasonic NDT methods in the case of aluminum/epoxy/aluminum assemblies. Different well identified levels of adhesion were obtained and qualified by mechanical tests. Several through-transmission ultrasonic techniques were used to evaluate different properties of these assemblies. Lamb waves and SH waves were used to investigate the variations in the adhesion level, which depends on the treatments carried out on the metal/epoxy interface [23,24]. As part of this study, the issue of surface roughness was addressed [9,25,26]. The present work is extending the results of the ANR ISABEAU project, with the case of dissymmetrical structures (metal/epoxy/composite).

A five-layer model, called interphases model [27-30], is used in the present study. This model consists in inserting two very thin layers between the substrates and the glue, to represent the substrate/adhesive transition of physical and chemical properties in the adhesive boundaries. Adhesion quality can then be characterized by the elasticity coefficients of this interphase layer [31].

The ultrasonic experimental evaluation is carried out successively on four samples. The first one is the reference sample for which the level of adhesion is high at both interfaces substrate/adhesive: an adhesive promotor is used to improve the adhesion on the metal interface and a total cross-linking of the epoxy adhesive (cross-linking rate of 100%). The second one is a sample with a good quality of bonding: the metallic surface is only degreased

and a partial cross-linking of the epoxy adhesive (cross-linking rate of 80%). For the two other samples, the quality of adhesion is degraded on a single side of the adhesive-substrate contact. This deterioration is ensured by the deposition of a thin layer of a release agent (called RA which is Cirex Si 041 WB) between adhesive and substrate, and on the other interface, the bonding quality remains good. The comparison between the experiment and the simulation assesses the adhesion level of the studied samples and also indicate the interface for which the adhesion quality is degraded. This is particularly useful to test bonded structures with access from only one side: this is often the case in industrial structures. To the author's knowledge, no work has been yet devoted to this last aspect.

2. Studied structure

We consider a three-layer structure as shown in Fig. 1, composed of an aluminum plate joined to a composite plate of carbon-epoxy by a thin layer of adhesive. For an orthotropic layer with the indicated crystallographic axes Ox_1 and Ox_2 (Fig.1), in which Lamb waves have a displacement field $\{u_1(x_1,x_2,t), u_2(x_1,x_2,t)\}$, according to the plane strain hypothesis, the following differential equations govern the elastic motion:

$$\frac{\partial}{\partial x_1}\left[C_{11}\frac{\partial u_1}{\partial x_1}+C_{12}\frac{\partial u_2}{\partial x_2}\right]+\frac{\partial}{\partial x_2}\left[C_{66}\left(\frac{\partial u_1}{\partial x_2}+\frac{\partial u_2}{\partial x_1}\right)\right]=\rho\ddot{u}_1$$

$$\frac{\partial}{\partial x_1}\left[C_{66}\left(\frac{\partial u_1}{\partial x_2}+\frac{\partial u_2}{\partial x_1}\right)\right]+\frac{\partial}{\partial x_2}\left[C_{21}\frac{\partial u_1}{\partial x_1}+C_{22}\frac{\partial u_2}{\partial x_2}\right]=\rho\ddot{u}_2$$

(1)

Since the composites are usually orthotropic, the differential equations of motion (Eq. 1), include from the nine elastic constant of an orthotropic material, the four independent elasticity constants C_{11}, C_{22}, C_{12} and C_{66} involved in the plane strain condition of Lamb waves [30]. The dispersion curves for Lamb waves in orthotropic materials can be computed as wavenumbers k (rad/m) functions of the frequency f or angular frequency $\omega = 2\pi f$ (rad/s), by assuming harmonic displacements and using the SAFE method [32]:

$$\frac{\partial}{\partial x_2}\left[\begin{bmatrix} C_{66} & 0 \\ 0 & C_{22} \end{bmatrix}\begin{bmatrix} \dfrac{\partial U}{\partial x_2} \\ \dfrac{\partial V}{\partial x_2} \end{bmatrix} + ik\begin{bmatrix} 0 & C_{66} \\ C_{12} & 0 \end{bmatrix}\begin{bmatrix} U \\ V \end{bmatrix}\right] + ik\begin{bmatrix} 0 & C_{12} \\ C_{66} & 0 \end{bmatrix}\begin{bmatrix} \dfrac{\partial U}{\partial x_2} \\ \dfrac{\partial V}{\partial x_2} \end{bmatrix}$$

$$+ \begin{bmatrix} \rho\omega^2 & 0 \\ 0 & \rho\omega^2 \end{bmatrix}\begin{bmatrix} U \\ V \end{bmatrix} = k^2 \begin{bmatrix} C_{11} & 0 \\ 0 & C_{66} \end{bmatrix}\begin{bmatrix} U \\ V \end{bmatrix}$$

(2)

The modal displacements U and V are along the Ox_1 and Ox_2 axis respectively (see Fig. 1). If the composite has orthogonal and identical plies [0°/90°] and the waves propagate along a principal axis, Ox_1 in this case, or Ox_3 along a perpendicular direction, the investigated phenomena remain the same, as for a transversally isotropic material.

Two layers (aluminum, adhesive) are assumed to be homogeneous and isotropic, characterized by their thickness (h_A and d), mass density (ρ_A and ρ_E) and the elasticity constants $\left\{C_{11}^{alu\,min\,um}, C_{66}^{alu\,min\,um}\right\}$ and $\left\{C_{11}^{epoxy}, C_{66}^{epoxy}\right\}$.

The composite layer is orthotropic, defined by thickness h_C, mass density ρ_C and the elasticity constants $\left\{C_{11}^{carbon-epoxy}, C_{22}^{carbon-epoxy}, C_{12}^{carbon-epoxy}, C_{66}^{carbon-epoxy}\right\}$. These parameters are given in Table 1.

In this work, three-layer samples with different adhesion levels are studied. The different adhesion levels are ensured at the time of their manufacture by different surface treatments, where the aim is either to reinforce or degrade the quality of the bonding (see details in Section 4.1). In the next section, a numerical model is developed to study the Lamb modes sensitivity to bonding quality and therefore to find the most sensitive modes to the adhesion level variation.

3.   Numerical study using interphases model

The objective is to develop a numerical model based on finite elements, for the propagation of Lamb waves in a metal/adhesive/composite structure. A SAFE (Semi Analytical Finite Element) model with one-dimensional finite elements of quadratic form functions is used to represent the equations (2). The appropriate mass and stiffness matrices of the model are implemented in the eigenvalue solver of a commercially available software [33], as shown on Fig. 1.

The boundary conditions between the three-layers are represented by the continuity of displacements and stresses for a perfect adhesion. The adhesion between the adhesive layer and the other two layers can be imperfect and several models exist in available literature for this purpose. The model used in this paper consists in two very thin elastic layers, one placed between the aluminum and adhesive layers and the other between the adhesive and the composite layers respectively [31]. These intermediary layers, which are called interphases in the following, have thicknesses of magnitude order of the surface roughness amplitudes. The elastic constants of the interphases are assumed to be equal to those of the adhesive for a perfect adhesion and smaller values for a degraded adhesion. This interphase model represents the transition of physical and chemical properties between the bulk adhesive layer and its properties at the surface of the substrate. At the same time, this model allows not only the continuity of displacements, but also the continuity of strains and stresses and consequently the continuity of normal/shear forces. The disadvantage of this model is the larger size of the SAFE model, which includes finite elements meshing the interphase layers. In this work, the two interphases between the metal and the adhesive, and respectively between the composite material and the adhesive, are considered as identical: isotropic, having the same mechanical properties and the same thickness (Fig. 1). The bonded assembly is thus modeled as a five-layer structure metal-interphase-adhesive-interphase-composite material. The thickness of each interphase is fixed to $h_{interphases}=1$ μm. This interphases thickness is commonly used for

such substrates, as can be found in other works on this subject [34,35]. For the investigated example, a number of 136 unidimensional finite elements of quadratic form functions were considered, with 2 elements per interlayer. The computation for 151 frequency values lasted 720 s on an I7 computer at 2.6 GHz. A perfect contact model requires only 70 elements and lasts 676 s on the same computer.

The change in physicochemical properties of the adhesion process can influence the quality of adhesion. To model the adhesion strength induced by the different surface treatments, the elastic constants of the interphase layers are defined as follows:

$$\begin{cases} C_{11}^{\text{int}\,erphase} = \alpha C_{11}^{epoxy} \\ C_{66}^{\text{int}\,erphase} = \alpha C_{66}^{epoxy} \end{cases} \quad \text{with } 0 \le \alpha \le 1$$

where the parameter α characterizes the adhesion level between the adhesive layer and the substrate: α=1 corresponds to the case of a perfect adhesion, while $\alpha = 0$ corresponds to a total delamination, the intermediate values describing different adhesion levels. The use of a single degradation parameter α is chosen to keep the model simple. Two parameters could be introduced in the model, one for each elastic coefficient, but this aspect remains to be developed in further studies.

This numerical model allows to calculate the eigenvalues solutions, associated to the above wave propagation equation and applying the boundary conditions: stress-free over the surfaces delimiting the three-layer and stress-displacements continuity for the four interfaces delimiting the two interphases layers. The dispersion curves of the Lamb modes are obtained from the eigenvalues solutions calculated for the selected frequency range, and for a given value of the parameter α. In order to validate the interphases model, we are testing two limit cases, which are: perfect adhesion and total delamination respectively.

The dispersion curves are shown in Fig. 2. The red dotted curves correspond to the dispersion curves plotted using the geometrical and material parameters values given in Table 1 and with α=1 for the two bonded interfaces.

This set of dispersion curves are compared to those obtained from a model with the layers in perfect c with α=1 for the two bonded interfaces is suitable to describe this structure with a perfect adhesion of the two interfaces (see blue dotted curves in Fig. 2).

Moreover, the case of total delamination was computed setting for $\alpha=10^{-5}$ (see Fig. 3). In this case, the dispersion curves of the bonded structure (red dots) correspond to those of each layer separately. These two extreme cases, prove the validity of the model.

In this work, we are particularly focusing on dissymmetric levels of adhesion with the aim to detect a possible delamination present at only one of the two interfaces. The numerical model is used to predict the effect on the dispersion curves when a high adhesion level is considered at the one interface, while a low level is imposed on the other interface. In Fig. 4, the dispersion curves of the aluminum/epoxy/carbon-epoxy structure are plotted in green for the case of a high bonding level on the aluminum/adhesive interface (corresponding to value of α equal to 1 and called $\alpha_{AL}=1$) and a low level of adhesion on the composite/adhesive interface (corresponding to $\alpha_C=10^{-5}$). In pink, the three-layer dispersion curves are plotted for the case of a bad bonding level on the aluminum interface ($\alpha_{AL}=10^{-5}$) and a high bonding level on the composite interface ($\alpha_C=1$).

These limit cases make it possible to observe the variation range of the wave numbers of the different modes propagating along the glued assembly. Indeed, when the stiffness of the interphase tends to zero, the guided modes propagating in the assembly tends to those propagating in a composite/adhesive bilayer or an aluminum/adhesive one (as will be seen later in Fig. 10). This figure is thus highlighting the modes that are very sensitive to the

interphase properties. Consequently, these modes can bring information about the quality of bonding.

4.   Experimental study

4.1.   Description of the experimental studied samples

The samples are three-layer structures composed of an aluminum plate of 4 mm thickness and of sufficiently large dimensions (300 mm x 200 mm) compared to the acoustic wavelengths (a few millimeters) glued to a carbon-epoxy composite plate of 1.8 mm thickness, same dimensions as the aluminum plate, by a thin layer of adhesive of 500 μm thickness. The adhesive used, is based on two epoxy system components: diglycidyl ether of bisphenol A (DGEBA, DER 331, Dow Chemicals) is cross-linked with an aliphatic diamine (jeffamine, D230, Aldrich). The epoxy and the diamine are mixed at room temperature with a stoichiometric ratio equal to 1.

In order to test the ability of our acoustic method to determine the adhesion level and to detect on which interface the quality of the adhesion is degraded, are used four different three-layer samples. The first assembly is made by degreasing the aluminum with isopropanol to remove all impurities and applying a chemical treatment with silane, which is an adhesion promoter and improves the level of adhesion between the aluminum and the adhesive, by creating covalent bonds of high strength. On the composite interface, the plate was directly glued after tearing the protective film. The tearing of the protective film creates a certain surface roughness of less than 15 μm on the interface to be glued, which improves the level of adhesion of this reference sample (called $Al_{DSi}E_{100}C_N$). The measure of the surface roughness is done with a surface roughness tester (manufacturer: Mitutoyo, model: SV-2100, resolution: 0.05 μm). The cross-linking of the epoxy adhesive is total (cross-linking rate of 100%). In

order to obtain this cross-linking level, the assembly is placed in a press (pressure: $1.5*10^5$ Pa) for 1 hour at 80 °C and then 3 hours at 160 °C.

In the second assembly, the aim is to obtain a medium-quality adhesion. The aluminum is only degreased with isopropanol. On the composite interface, the plate is directly glued after tearing the protective film. The structure is then cured at room temperature for one week in order to obtain a partial cross-linking (80% conversion). This sample is called $Al_DE_{80}C_N$.

In the third assembly, the aim is to highly degrade the quality of the aluminum/glue interface. First of all, the aluminum interface is degreased. Afterwards, a RA thin layer is deposited on the aluminum interface before making the assembly and infusing the adhesive. The composite interface is glued directly without any treatment. The cross-linking rate of the epoxy adhesive is 100%. This sample is called $Al_{DRA}E_{100}C_N$.

In the fourth assembly, an opposite treatment of the third assembly is done, i.e. the aluminum interface is degreased and then silane is applied on it, but a thin layer of RA is applied on the composite interphase. The cross-linking rate of the epoxy adhesive is 100% too. This sample is called $Al_{DSi}E_{100}C_{RA}$. The nomenclature of the studied samples is summarized in Table 2.

4.2. *Experimental protocol and signal processing*

The experimental study is based on the use of a contact transducer (manufacturer: Krautkramer, central frequency of 2.25 MHz) for the generation of Lamb waves, and on detection by laser interferometry (manufacturer: Polytec, model: OFV-5000, sensitivity of 20 V/(m s^{-1})) [36], as shown on Fig. 5. The excitation signal is a pulse of 300 ns duration and large bandwidth, the aim is to generate different Lamb modes. The transducer is placed on a Plexiglas wedge inclined ($\theta = 25°$) with regard to the plate surface of aluminum. This method, called the wedge method, is the most used for the generation of guided waves by

piezocomposite contact transducers (see for examples [37] and [38]). The Snell's law at the interface between the wedge and the sample enables to calculate the wavenumber k versus the

frequency f : $k = \dfrac{2\pi \sin\left(\dfrac{\pi}{180}\theta\right)}{C_{T\,Plexiglas}} f$ where $C_{T\,Plexiglas} = 1340\ m.s^{-1}$ is the transversal velocity in

Plexiglas and θ is the angle in degree. In the frequency-wavenumber space, this equation is a straight line. The excited modes are the modes around this straight line. The excited signal is a pulse and the transducer has a wide frequency bandwidth (frequency bandwidth at -6 dB equal to 2 MHz) so the modes are excited over a large area around this straight line. The wedge angle is chosen so as to generate a maximum number of modes on the studied frequency bandwidth.

The coupling between the transducer and the wedge and between the wedge and the bonded assembly is ensured by a water-based gel, which provides a good acoustic coupling and so a better transmission of the waves generated into the studied structure. The time varying signals (i.e. the normal velocity at the surface) due to the propagating Lamb waves are measured by the Laser velocimeter which is translated in the propagation direction, by steps of 0.1 mm, over 70 mm distance. For each position, the acquisition of the signal is carried out over 100 μs duration, corresponding to 10000 time samples. The data are gathered in a matrix called the time-position matrix, which is therefore of 10000 rows and 700 columns. A representation in color levels of this matrix is given in Fig. 6a. An example of the temporal signal recorded at a given x-position (here x=20 mm) is given in Fig. 6b. Spatial and temporal Fast Fourier Transform (FFT) are performed on the time-position matrix. The temporal FFT is performed on 262144 points with a frequency step of $\Delta f = 381.46\ \text{Hz}$. The spatial FFT is performed on 32768 points with a wavenumber step of $\Delta k = 1.92\ \text{m}^{-1}$. The aim is to respect the Nyquist-Shannon sampling theorem, which is largely the case in this study.

The minimum sampling rate is in time about $2 \cdot 10^{-7}$ s and in space about $0.5 \cdot 10^{-3}$ m. We use the zero-padding technique to improve the localization of the maxima of the spectrum. The result of the 2D FFT [32] provides the experimental dispersion curves in the wavenumber-frequency space, for comparison against those obtained from the numerical model.

5. Results and discussion

The experiments are performed in the same conditions for all samples (i.e. same transducer, PMMA wedge, excitation signal, acquisition conditions and signal processing). The objective is to experimentally detect a different behavior in the propagation of the Lamb waves which indicates whether a delamination is present.

In Fig. 7, the experimental dispersion curves for the reference sample $Al_{DSi}E_{100}C_N$ are plotted in color levels. A direct problem is done to superpose the numerical dispersion curves with the experimental ones. At each frequency, the difference between these two sets of dispersion curves is calculated: $\varepsilon = \dfrac{\left| k_{numerical} - k_{experimental} \right|}{k_{experimental}}$. The best fit (error $\varepsilon = 1.1\%$) is obtained for the combination of $\alpha = \alpha_{Al} = \alpha_C = 1$ (in red dots), reflecting the adhesion level of this sample. The case $\alpha_{Al} = \alpha_C = 1$ corresponds to values of the C_{11} and C_{66} of the interphases equal to that of the glue and thus corresponds to a perfect coupling between the two considered layers. In other words, it confirms the high level of adhesion between the two substrates.

The experimental result for the $Al_D E_{80} C_N$ sample (i.e. medium-quality adhesion on the aluminum/adhesive interface and good adhesion on the composite/adhesive interface) is shown in Fig. 8.a. The comparison with the numerical model furnishes as best fit (error $\varepsilon = 1.0\%$) the combination of $\alpha_{AL} = 10^{-3}$ and $\alpha_C = 1$, reflecting the adhesion level of this sample.

To confirm this result, we zoom on modes sensitive to the level of adhesion (see Fig. 8.b): we note that the experimental signal superposes to the numerical model with the adhesion parameters $\alpha_{AL}=10^{-3}$ and $\alpha_C=1$ (blue crosses) and not with the case of a perfect adhesion (red circles).

The experimental result for the $Al_{DRA}E_{100}C_N$ sample (i.e. bad adhesion on the aluminum/adhesive interface and good adhesion on the composite/adhesive interface) is shown in Fig. 9. The comparison with the numerical model furnishes as best fit (error $\varepsilon = 0.84\%$) the combination of $\alpha_{AL}=1.1\cdot10^{-5}$ and $\alpha_C=1$ (blue dots), reflecting the adhesion level of this sample. Because the excitation and the measurements are on the aluminum surface and the presence of the RA is on the aluminum/adhesive interphase, the Lamb waves propagation is only possible in the aluminum plate. This explains the excellent superposition of experimental values on the dispersion curves of a single, 4 mm thick aluminum plate, shown in pink on Fig. 9.

For the fourth sample ($Al_{DSi}E_{100}C_{RA}$), the numerical dispersion curves for $\alpha_{AL}=1$ and $\alpha_C=0.8\cdot10^{-5}$, plotted in green, are well superimposed (error $\varepsilon = 0.81\%$) on the experimental results (see Fig. 10). We can conclude that the presence of the RA on the composite surface causes a high degradation of adhesion. This explains why we end up with an aluminum/epoxy bilayer structure, as can be seen when its numerical dispersion curves (in yellow), are superimposed on the experimental ones. It is thus possible to experimentally identify the degradation of the bonding quality on the composite interface.

These results show that, generating guided Lamb waves which propagate through the whole structure of the aluminum/adhesive/composite assembly, and by performing the excitation as well as the observation on only one accessible surface of the three-layer (here on

the aluminum interface), one can detect which interface is degraded, the nearest or the farthest with respect to excitation-observation surface.

6. Conclusions

The propagation of Lamb modes in a three-layer structure (aluminum/adhesive/carbon-epoxy composite) has been considered. The predicted dispersion curves for the Lamb modes in the bonded structures were first determined using the SAFE method (1D model). The link between substrate and glue was modeled by a very thin layer called interphase. Various samples with very different adhesion levels, indicated by the parameter α ($\alpha=0\ldots1$) have been investigated and a data base of dispersion curves has thus been obtained. Experiments were then carried out to determine experimental dispersion curves. On each experimental result, numerically computed Lamb dispersion curves were superimposed and the most adequate value of the adhesion quality parameter α for each interphase was determined. The different samples quality could be thus identified by this method. And in particular, it was possible to identify on which side the quality of the adhesion was degraded (metal/adhesive or composite/adhesive interface).

The present results could be used as basis for quality control in the manufacturing process of bonded structures, in which case the technological process could be monitored over large areas. This is particularly useful to test bonded structures with access from only one side, which is often the case in industrial structures.

References

[1] Da Silva L, Ochsner A, Adams R. Handbook of Adhesion Technology I, II. Berlin: Springer; 2011.

[2] Brockmann W, Geiß PL, Klingen J, Schröder KB. Adhesive Bonding: Materials, Applications and Technology. New York: John Wiley & Sons; 2009.

[3] Zhou YN, Breyen MD. Joining and Assembly of Medical Materials and Devices. London: Elsevier; 2013.

[4] Auld BA. Acoustic Fields and Waves in Solids I. New York: J Wiley & Sons; 1973.

[5] Brekhovskikh LM, Godin OA. Acoustics of Layered Media I. Berlin: Springer; 1990.

[6] Cheeke JD. Fundamentals and Applications of Ultrasonic Waves. Boca Raton, Florida: CRC Press LLC; 2002.

[7] Guyott CCH, Cawley P. The ultrasonic vibration characteristics of adhesive joints. J Acoust Soc Am 1988;83:632-40.

[8] Nagy PB, Adler L. Nondestructive evaluation of adhesive joints by guided waves. J Appl Phys 1989;66(10):4658-63.

[9] Gauthier C, El-Kettani MEC, Galy J, Predoi M, Leduc D, Izbicki JL. Lamb waves characterization of adhesion levels in aluminum/epoxy bi-layers with different cohesive and adhesive properties. Int J Adhes Adhes 2017;74:15-20.

[10] Hernando Quintanilla F, Lowe MJS, Craster RV. Modeling guided elastic waves in generally anisotropic media using a spectral collocation method. J Acoust Soc Am 2015;137(3):1180-94.

[11] Yew CH, Weng X. Using ultrasonic SH waves to estimate the quality of adhesive bonds in plate structures. J Acoust Soc Am 1985;77:1813-23.

[12] Le Crom B, Castaings M. Shear horizontal guided wave modes to infer the shear stiffness. J Acoust Soc Am 2010;127:2220-30.

[13] Adams R, Drinkwater B. Nondestructive testing of adhesively-bonded joints. NDT&E Int 1997;30:93-8.

[14] Lowe M, Cawley P. The applicability of plate wave techniques for the inspection of adhesive and diffusion bonded joints. J Nondestr Eval 1994;13:185-200.

[15] Kundu T, Maslov K. Material interface inspection by Lamb waves. Int J Sol Struct 1997;34:3885-901.

[16] Coulouvrat F, Rousseau M, Lenoir O, Izbicki JL. Lamb-type waves in a symmetric solid-fluid-solid trilayer. Acta Acust united Ac 1998;84:12-20.

[17] Heller K, Jacobs LJ, Qu J. Characterization of adhesive bond properties using Lamb waves. NDT&E Int 2000;33:555-63.

[18] Barros S, Gama A, Rousseau M, Collet B. Characterization of bonded plates with Lamb and SH waves using a quasi-static approximation. Latin Am J Sol Struct 2004;1:379-99.

[19] Brotherhood C, Drinkwater B, Dixon S. The detectability of kissing bonds in adhesive joints using ultrasonic techniques. Ultrasonics 2003;41:521-29.

[20] Lanza di Scalea F, Rizzo P. Propagation of ultrasonic guided waves in lap-shear adhesive joints: case of incident A_0 Lamb wave. J Acoust Soc Am 2004;115:146–57.

[21] Allin J, Cawley P, Lowe M. Adhesive disbond detection of automotive components using first mode ultrasonic resonance. NDT&E Int 2003;36:503-14.

[22] Malinowski P, Wandowski T, Ostachowicz W. Characterization of CFRP using piezoelectric transducer and laser vibrometry. 10th int. conf. on damage assessment of structures. Dublin, Ireland 2013.

[23] Siryabe E, Rénier M, Meziane A, Galy J, Castaings M, Apparent anisotropy of adhesive bonds with weak adhesion and non-destructive evaluation of interfacial properties. Ultrasonics 2017;79:34-51.

[24] Gauthier C, Galy J, Ech Cherif El Kettani M, Leduc D, Izbicki JL. Evaluation of epoxy crosslinking using ultrasonic Lamb waves. Int J Adhes Adhes 2018;80:1-6.

[25] Potel C, Bruneau M, Foze N'Djomo L, Leduc D, Echcherif Elkettani M, Izbicki JL. Shear horizontal acoustic waves propagating along two isotropic solid plates bonded with a non-dissipative adhesive layer: effects of the rough interfaces. J Appl Phys 2015;118:224904.

[26] Ech Cherif El Kettani M, Leduc D, Potel C, Bruneau M, Foze Ndjomo L, Predoi M. Effects of the interface roughness in metal-adhesive-metal structure on the propagation of SH waves J Acoust Soc Am 2017;6:4591-9.

[27] Lavrentyev AI, Rokhlin SI. Ultrasonic spectroscopy of imperfect contact interfaces between a layer and two solids. J Acoust Soc Am 1998;103(2):657-64.

[28] Drinkwater BW, Castaings M, Hosten B. The measurement of A_0 and S_0 Lamb wave attenuation to determine the normal and shear stiffnesses of a compressively loaded interface. J Acoust Soc Am 2003;113(6):3161-70.

[29] Her SC, Lin YC. Assessment of adhesive bond strength using the ultrasonic technique. J Adhes 2014;90(5-6):545-54.

[30] Hosten B, Castaings M. Finite elements methods for modeling the guided waves propagation in structures with weak interfaces. J Acoust Soc Am 2005;117(3):1108-13.

[31] Kinloch AJ, Little MSG, Watts JF. The role of the interphase in the environmental failure of adhesive joints. Acta Mater 2000;48(18-19):4543-53.

[32] Predoi MV, Castaings M, Moreau L. Influence of material viscoelasticity on the scattering of guided waves by defects. J Acoust Soc Am 2008;124(5):2883–94.

[33] COMSOL Multiphysics Modeling Software, User Manual. COMSOL Inc; 2018.

[34] Moidu AK, Sinclair AN, Spelt JK. Nondestructive characterization of adhesive joint durability using ultrasonic reflection measurements. J Res Nondestruct Eval 1999;11(2):81-95.

[35] Monchalin JP. Optical detection of ultrasound. IEEE Trans Ultrason Ferroelectr Freq Control 1986;33:485-99.

[36] Alleyne D, Cawley P. A two-dimensional Fourier transform method for the measurement of propagating multimode signals. J Acoust Soc Am 1991;89(3):1159-68.

[37] Viktorov I. Rayleigh and Lamb waves. New York: Plenum 1967.

[38] Alleyne D, Cawley P. Optimization of Lamb wave inspection techniques. NDT&E Int 1992;25(1):11-22.
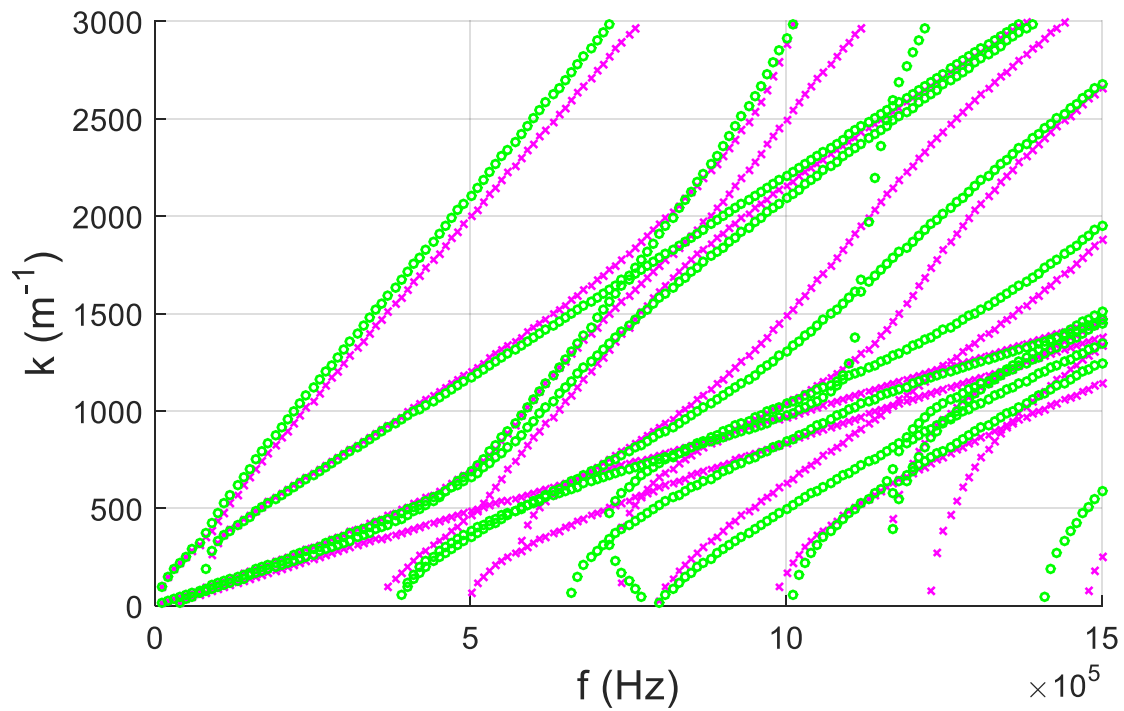
Fig. 1

Fig. 2

Fig. 3

Fig. 4

Fig. 5

Contact
Transducer +
plexiglass
wedge

Laser Velocimeter

Computer

Oscilloscope

Impulse
generator
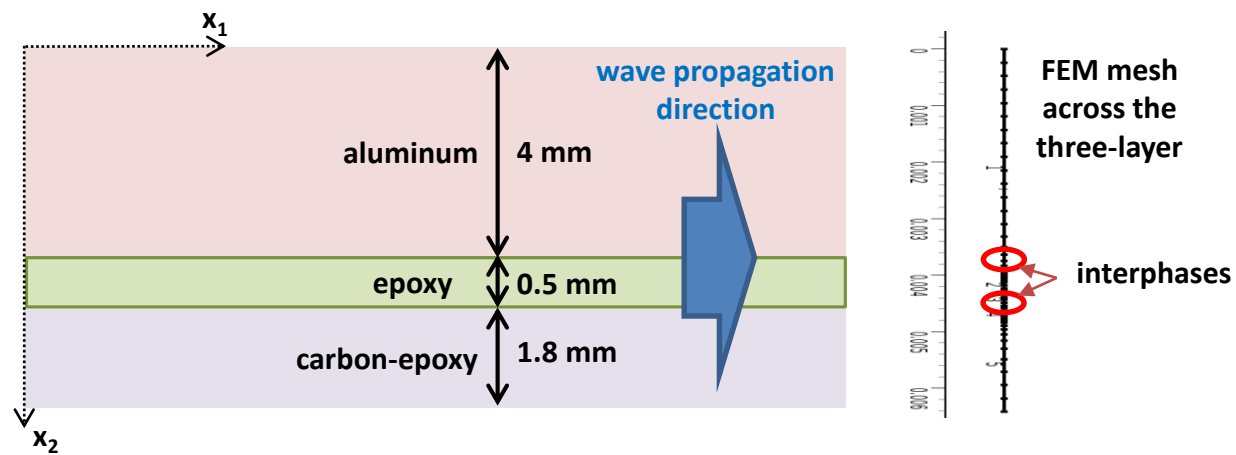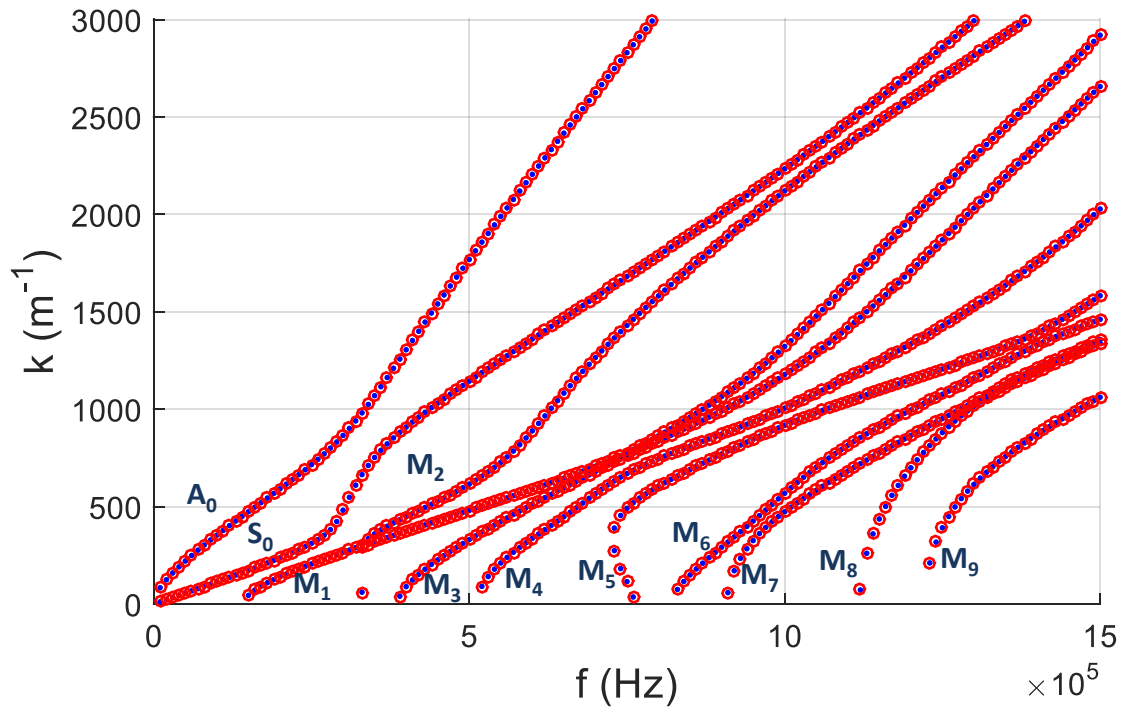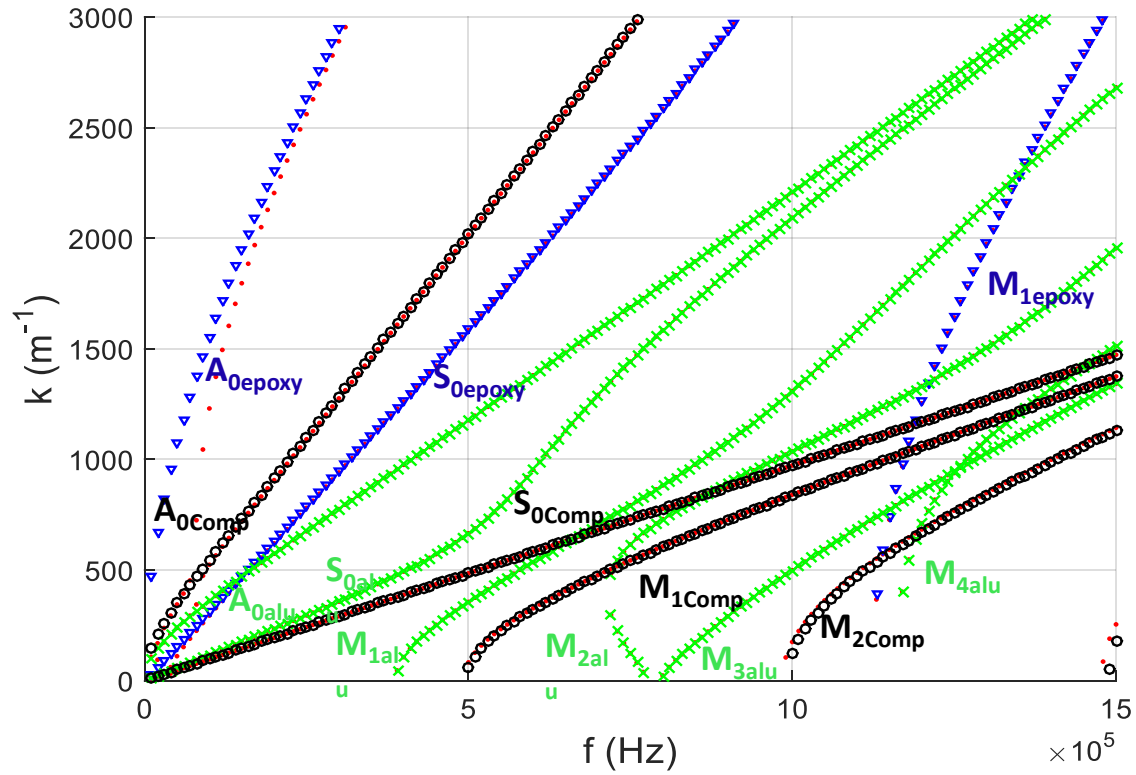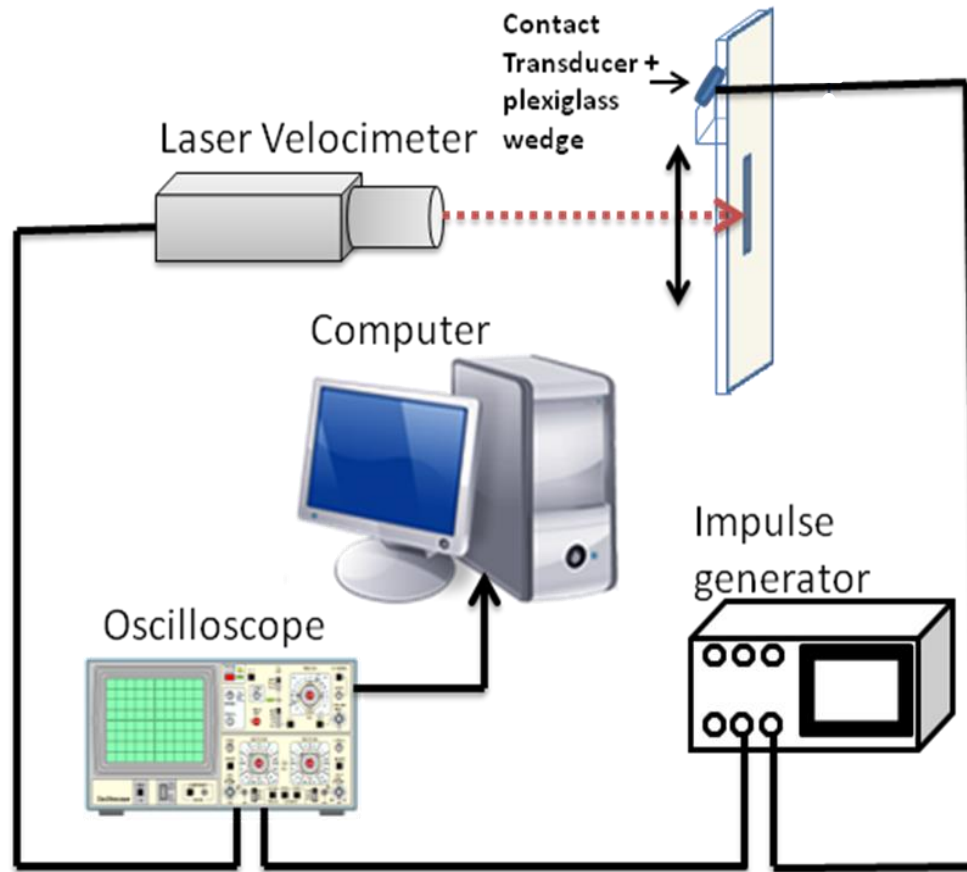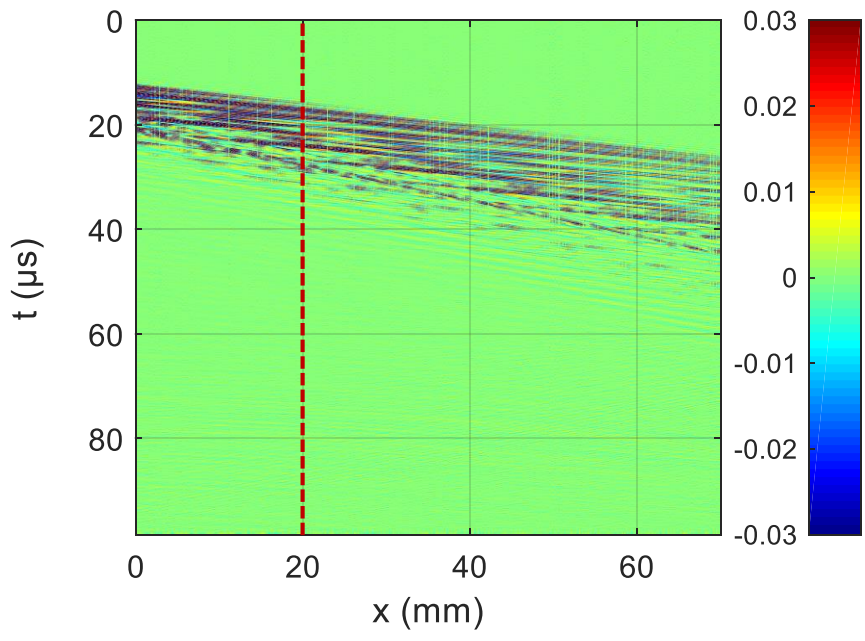
Fig. 6. (a)
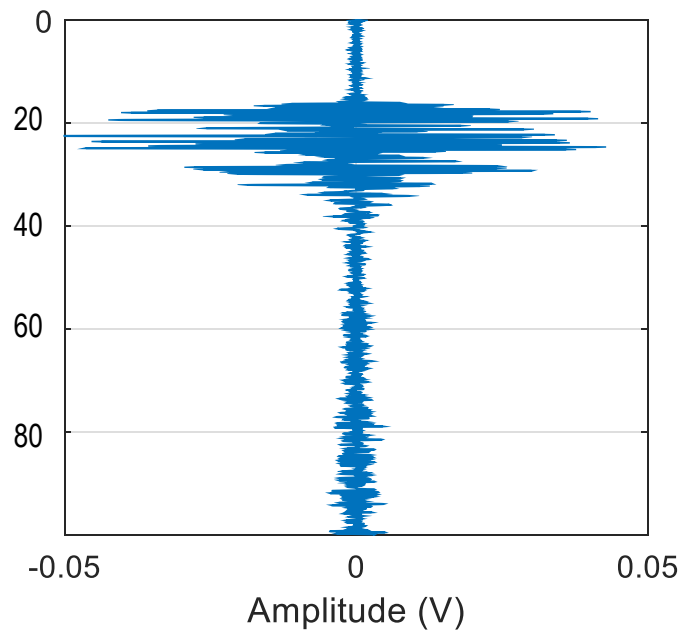
Fig. 6. (b)

Fig. 7
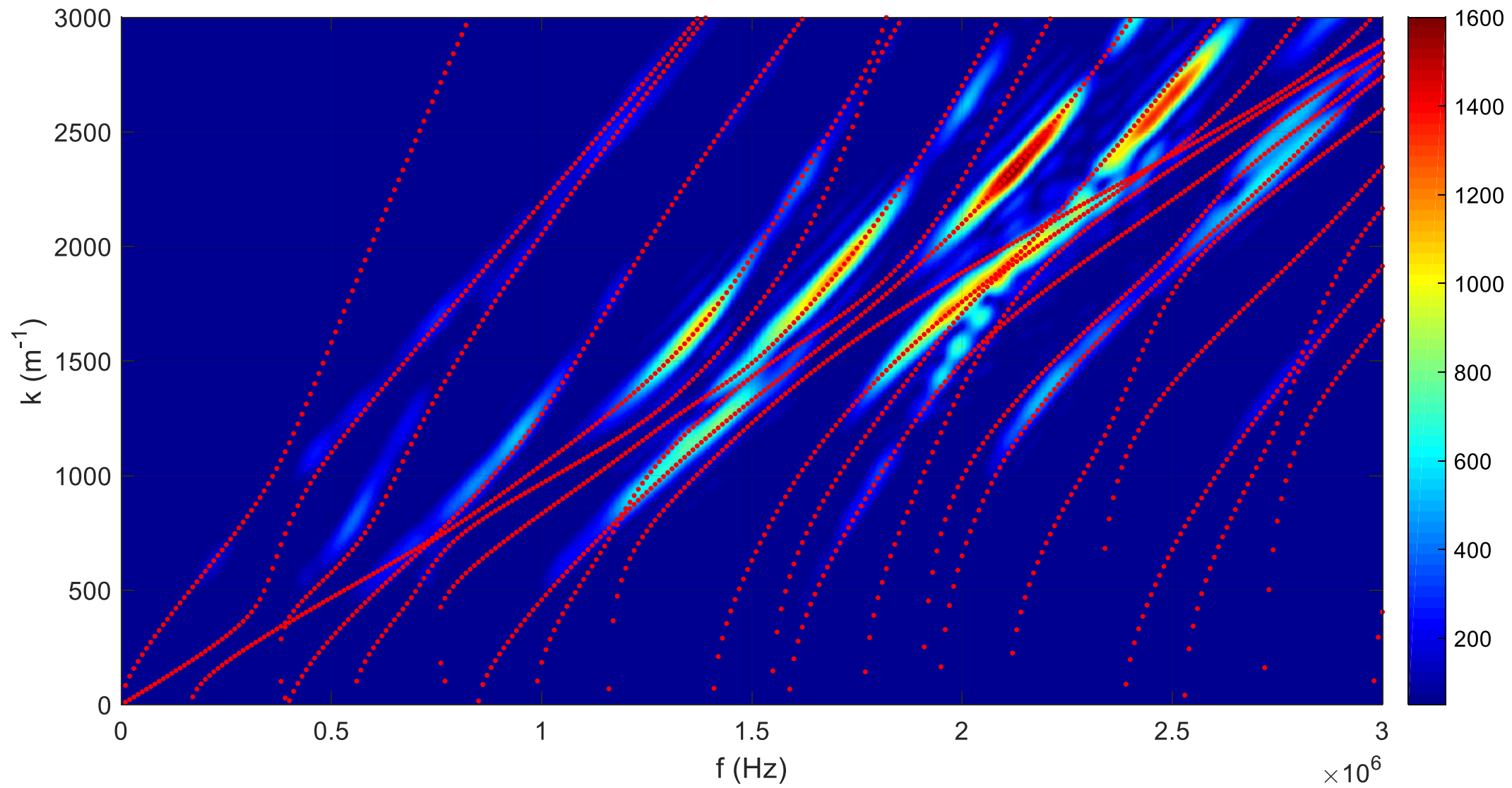
Fig. 8.a
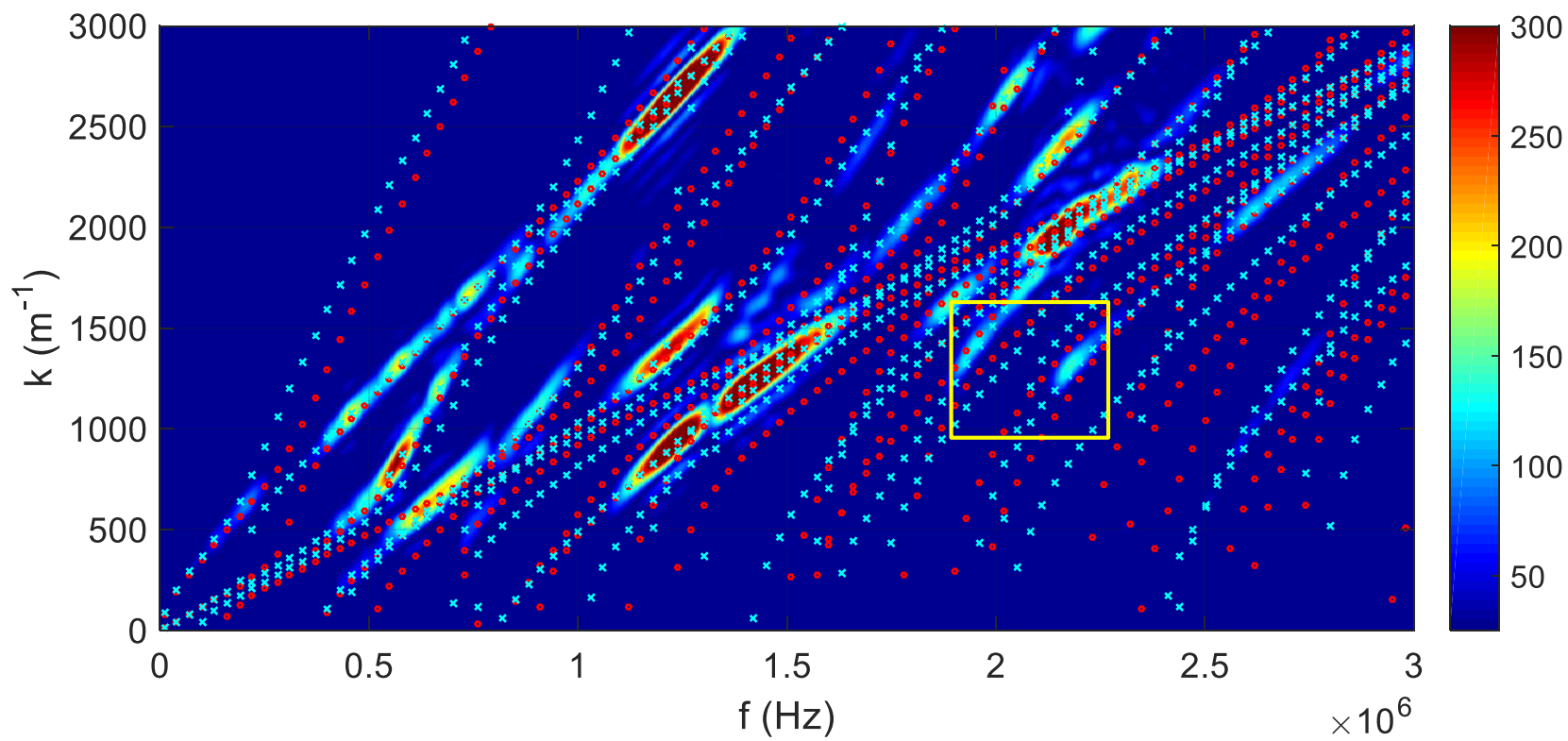
Fig. 8b
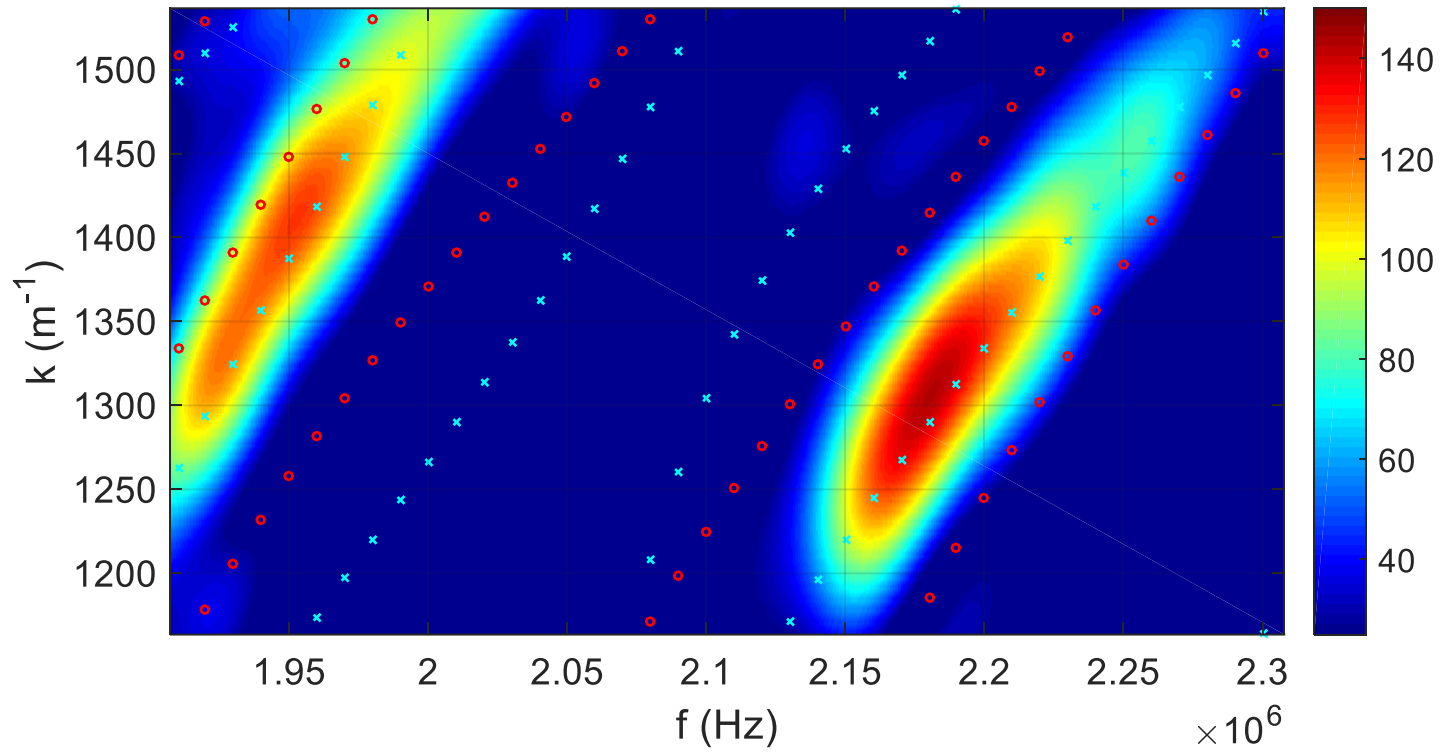
Fig. 9
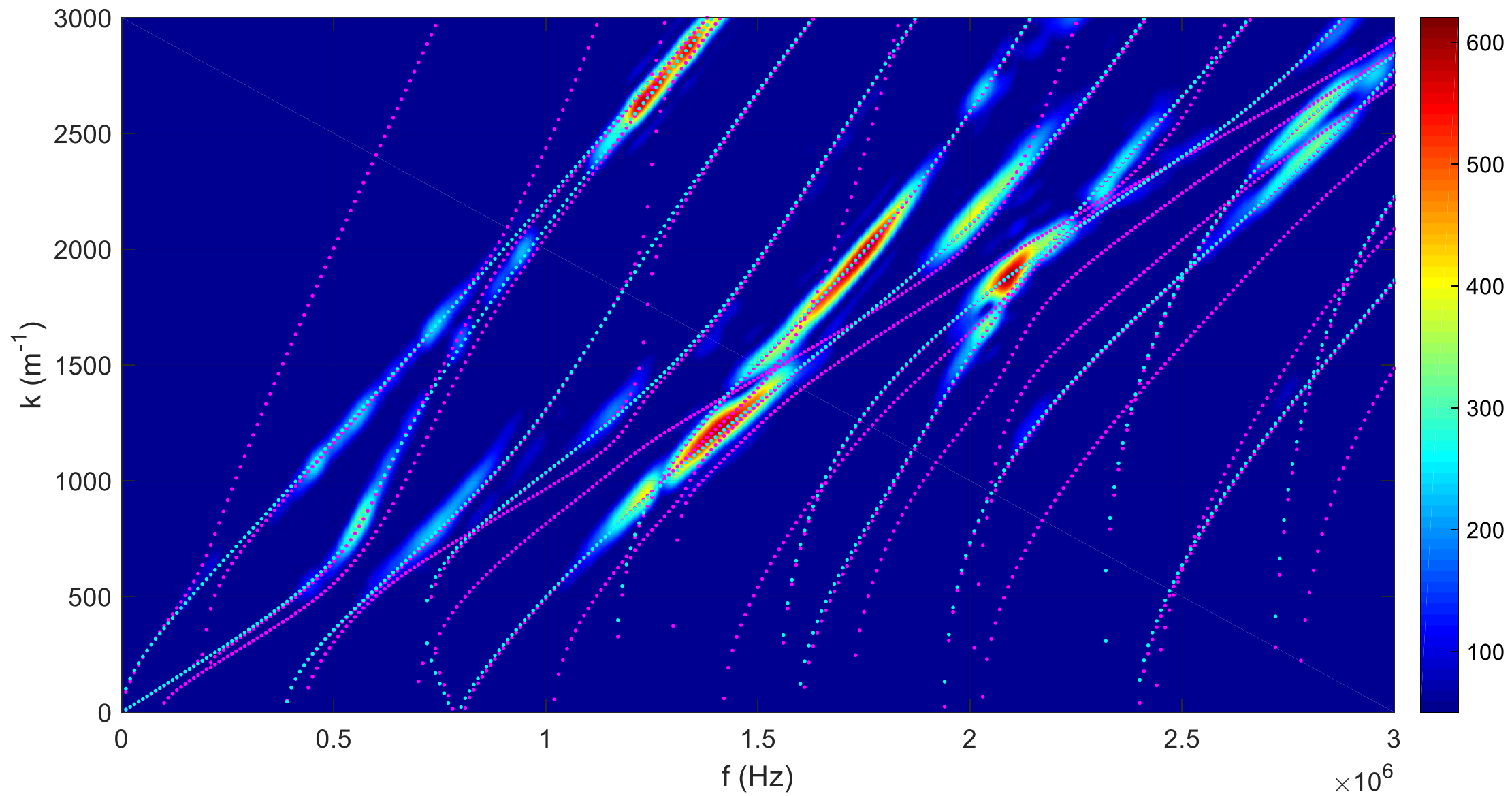
Fig. 10
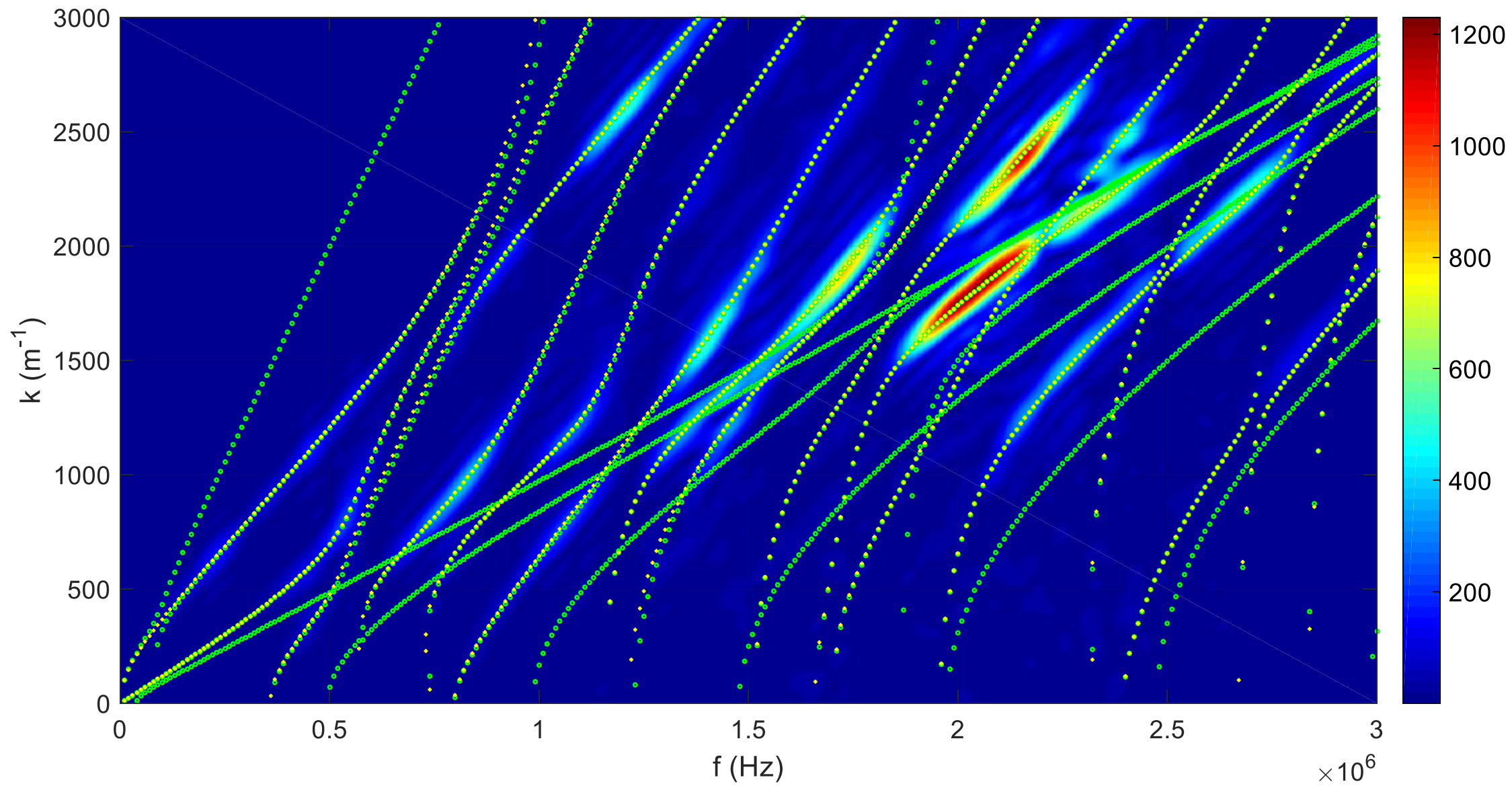
material	ρ (kg/m³)	C_{11} (GPa)	C_{12} (GPa)	C_{22} (GPa)	C_{66} (GPa)	thickness (mm)
aluminum	2800	113.97	60.15	113.97	26.91	4
epoxy	1160	6.94	4.02	6.94	1.46	0.5
carbon-epoxy composite	1700	72.31	8.55	16.89	4.87	1.8

Table 1. Physical and geometrical parameters of each studied layer.

sample	aluminum treatment	composite treatment	epoxy conversion
$Al_{DSi}E_{100}C_N$	degreased and silanized	none	100 %
$Al_D E_{80} C_N$	degreased	none	80 %
$Al_{DRA}E_{100}C_N$	degreased and release agent	none	100 %
$Al_{DSi}E_{100}C_{RA}$	degreased and silanized	release agent	100 %

Table 2. Set of manufactured samples.